MIND and TASD

Etam NOAH - Geneva University

March 26, 2014

On behalf of WP8.5.2 collaborators

Some relevant future neutrino detectors

MIND at a Neutrino Factory

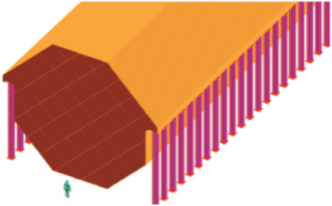

LBNO Far Detector

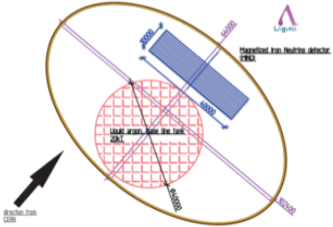

SuperBIND: MIND for νSTORM

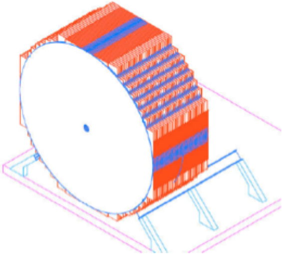

LBNO Near Detector

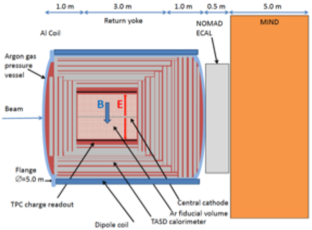

Short baseline ν: ICARUS/NESSIE: SPSC-2012-010... νSTORM/100 T: SPSC-EOI-009...

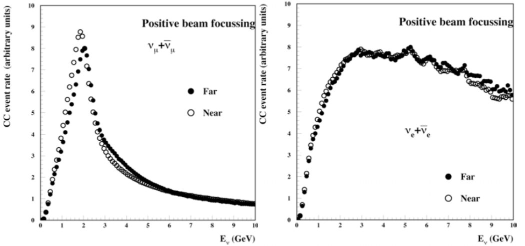

Figure 3: Muon (left) and electron (right) neutrino CC interaction spectra, at the Near and Far positions, arbitrary normalization.

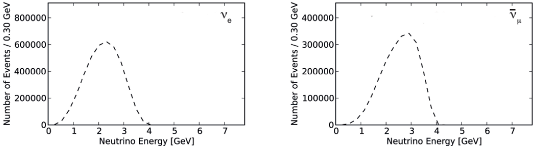

Hyper-Kamiokande ν_μ events at a near detector

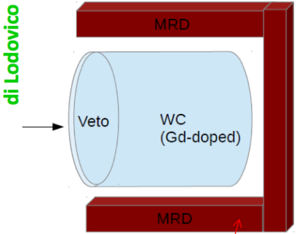

- **1kton** – D: 10.8m H: 10.8m
- **2kton** – D: 11m H: 22m
- **4kton** – D: 22m H: 11m
- **8kton** – D: 22m H: 22m

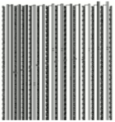

To measure energy, angle and production point of muon from CC interactions

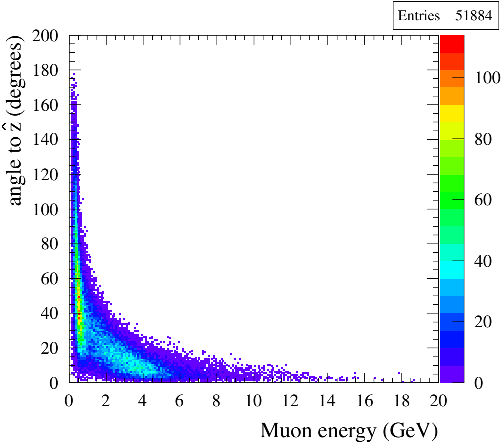

LBNO near detector ν_μ event rates

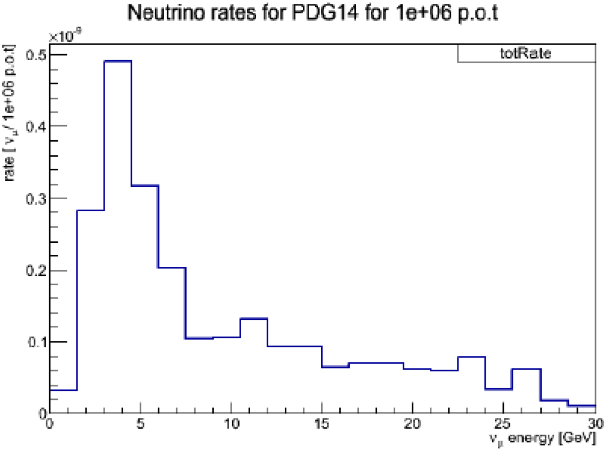

Motivation for AIDA MIND and TASD prototypes

- Magnetised Iron Neutrino Detector (MIND):
  - Muon charge identification, for wrong sign muon signature of a neutrino oscillation event: golden channel at a NF: requires correct sign background refection of 1 in 10^4: test beam 0.8 to 5 GeV/c;
  - Hadronic shower reconstruction for identification of charged current neutrino interactions and rejection of neutral current n.i.: test beam protons/pions 0.5 to 9 GeV/c.
- Totally Active Scintillating Detector (TASD):
  - Stopping properties of pions and muons up to 200 MeV/c (MICE EMR);
  - Electron and muon charge separation inside a magnetic field, in particular electron charge ID in electron neutrino interaction for the platinum channel at a neutrino factory: 0.5 to 5 GeV/c.

TASD at MICE: The Electron-Muon Ranger (EMR)

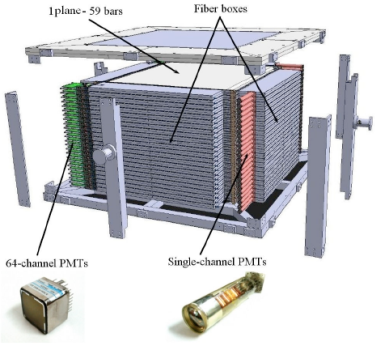

- 1 m^3 active volume;
- 24 modules: 1 module = one X + one Y plane.

- 59 triangular scintillator bars per plane → 2832 bars;
- light is collected by WLS fiber and transported to PMTs by clear fiber light guide;
- Different readout scheme at either end of every bar:
  - At one end, total energy per plane is detected by sending light from all bars to one single channel PMT (PHILIPS);
  - At other end, energy in every bar is detected by sending light from each into a fiber bundle connected to 64-ch PMT (HAMAMATSU).

TASD EMR electronics

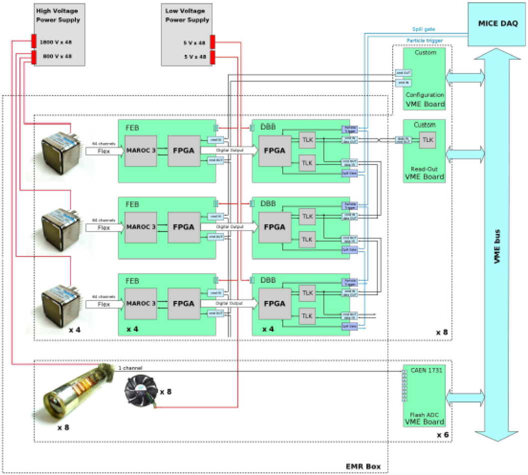

- The EMR has dual readout;
- On one side of a given plane, a 1-ch PMT reads the total energy deposited in the plane. Eight 1-ch PMTs are readout by one fADC (CAEN V1731), a total of 6 fADC;
- One the other side of a given plane, a 64-ch PMT reads the energy deposited in each bar. These PMTs are readout with custom electronics.

TASD EMR Front End Board

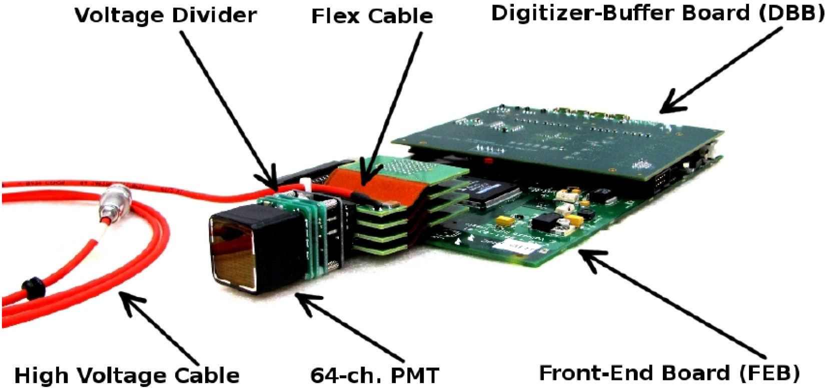

The Front-End Board (FEB) is designed to readout the 64-ch. PMT. It hosts a MAROC ASIC that amplifies, discriminates and shapes all input signals. Pulse height information can be extracted at low rate (during calibration with cosmics). Time over threshold information is directed to a piggy-back buffer board.

The Digitizer-Buffer Board (DBB) receives signals from FEB and stores them in buffer memory. MICE beam is made of 1ms spills every second. Every spill is composed of hundreds of particles. All interactions of these particles are stored in DBB and transferred to PC at the end of a spill.

Scintillator bars, WLS fiber and connectors

- ~3000 bars seen here;
- Major issue with quality of optical chain;
  - Connectors;
  - WLS light guide from St. Gobain;
  - Fiber polishing
- Old config. B1:attenuation in fiber = 48%. Cracks in fiber.
- New config. B2+C2(insertion loss) = 38%.

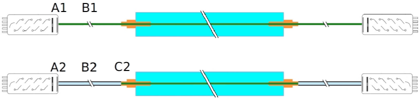

Fiber polishing

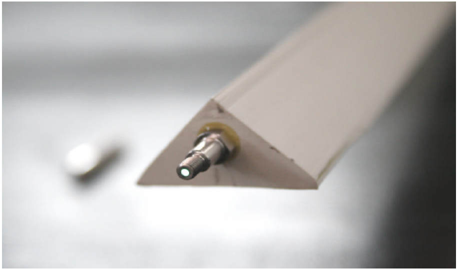

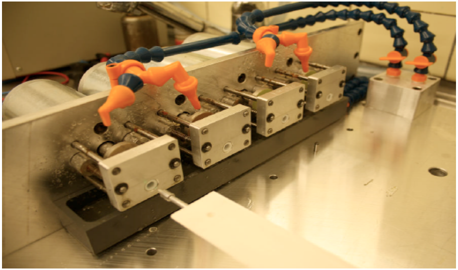

- 6000 connectors polished incl. spares.
- Polishing jig consists of 4 motors equipped with different polishing papers from coarse to fine grade.

WLS-to-clear fiber light guide coupling

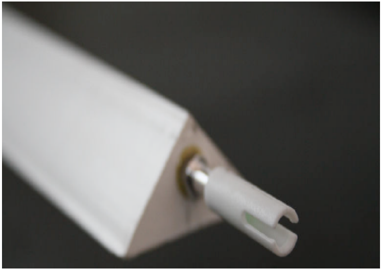

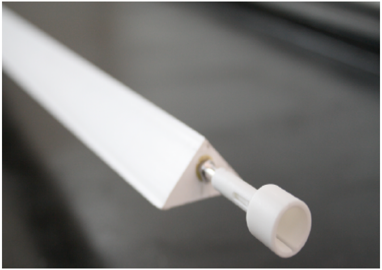

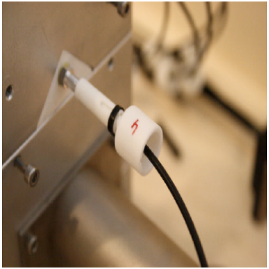

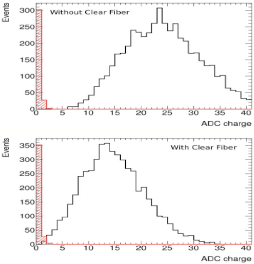

- Light attenuation in clear fiber and connector measured to be 38% mainly due to insertion losses.

Insertion of bars into module mechanics

Cabling of clear fibers

Clear fiber tray

FEB installation

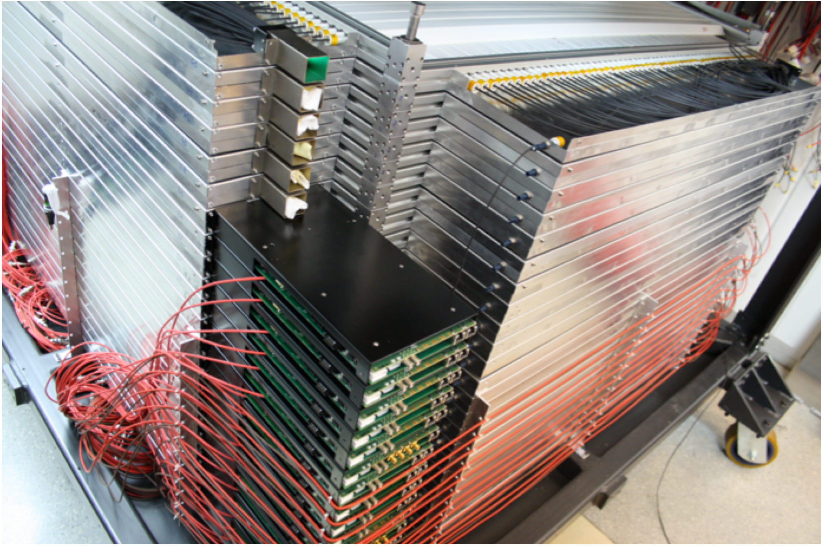

Closing the box

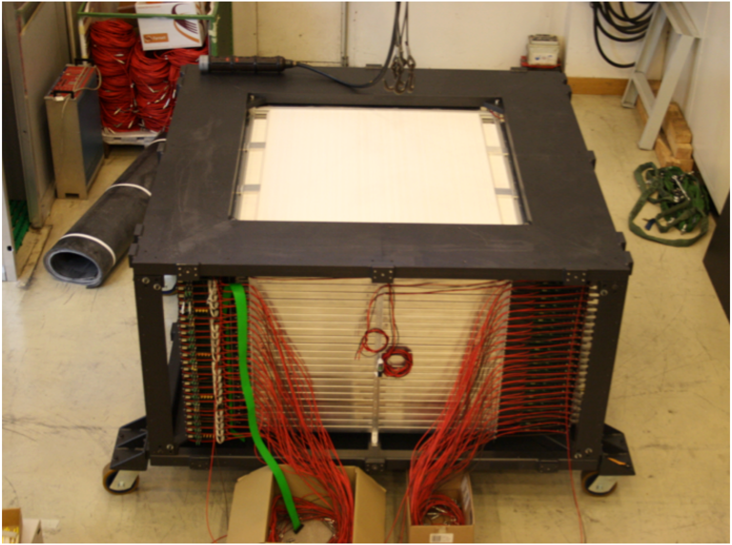

Final cabling

Transport from Geneva September 2013

Calibration with cosmics: Jan. 2014

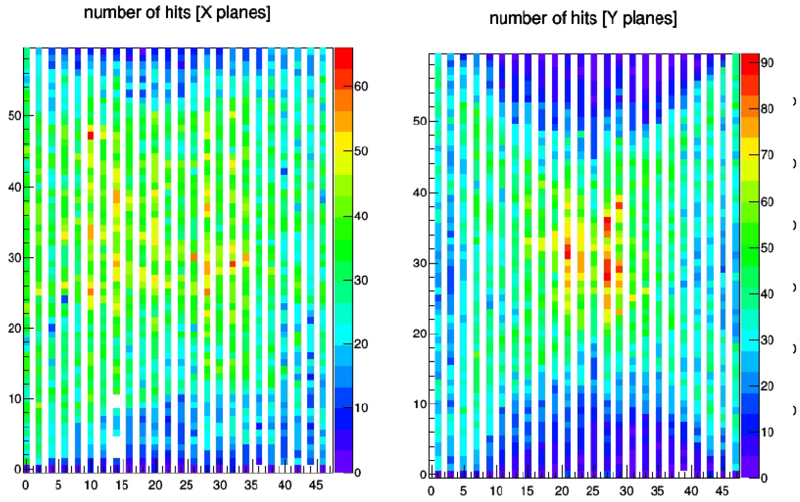

Crosstalk sources I/III

1) Fibers aperture angle

- A single fiber can shine on several channels of the MAPM
- Single cladding fiber of diameter $\o_F = 1.5mm$
- Distance between two channels of the MAPM $\Delta x_C = 2.3mm$

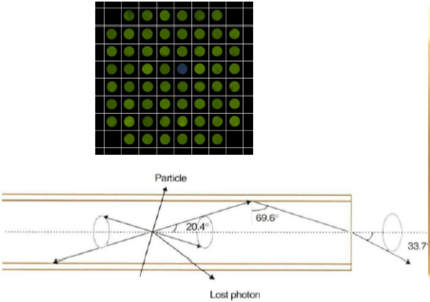

Figure : Mask, SC fiber

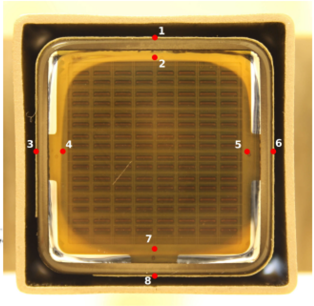

Figure : MAPM front

Crosstalk sources II/III

2) Electronic crosstalk

- A photo-electron can leak from a dynode to an adjacent multiplying structure
- The bigger the initial photo-production, the more likely the leak

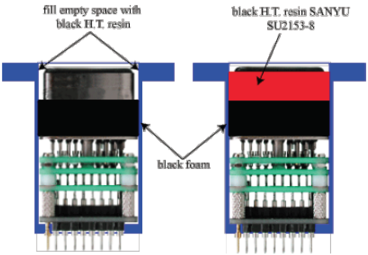

Figure : MAPM lateral view

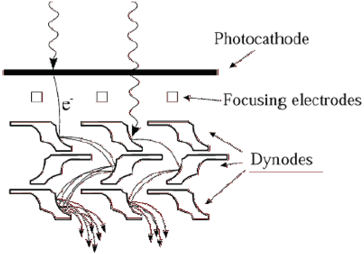

Figure : Electron leak

Crosstalk sources III/III

3) Mask misalignment
4) Irregular spacing between the fibers
   - Fibers can be glued irregularly in mask, getting them closer to the edge of their corresponding channel in the MAPM

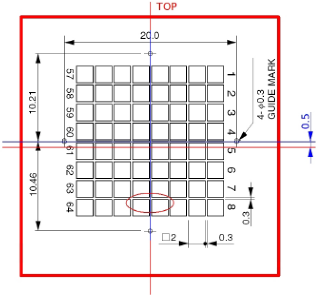

Figure : MAPM measurements

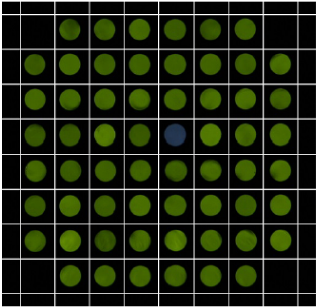

Figure : Mask, fibers positions

Crosstalk analysis I/III

For this analysis, we focus on Channel 0

- Channel 0 on the MAPM corresponds to a fiber connected to a tunable LED pulser
- For each hit in channel 0, we measure the Time over Threshold in the surrounding channels

→ No other effects, clean measurements

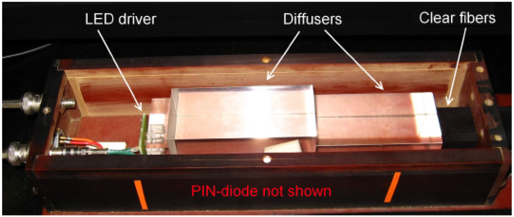

Figure : LED Driver

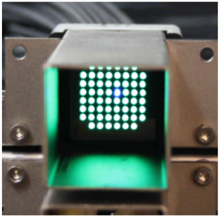

Figure : Bright blue channel 0

Crosstalk analysis II/III

For each plane and each channel surrounding channel 0, we measure two main parameters

- The **ratio** of the ToT measured in that channel over the ToT in channel 0, that is $Ratio = \frac{ToT_i}{TOT_0}$
- The **rate**, i.e. the percentage of the time an adjacent channel is lit along with channel 0, that is $Rate = \frac{N_i}{N_0}$

The channels are named after the cardinal points

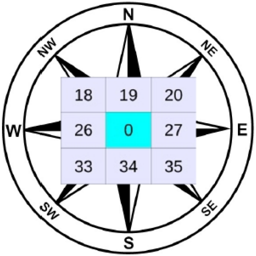

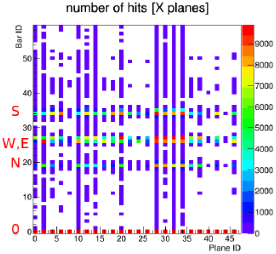

Crosstalk analysis III/III

Integrated crosstalk rates for a given plane

- At MIP level, the crosstalk is almost inexistent with percentage of the order of 0.5% or less
- At high energy deposition, the levels almost reach 100%

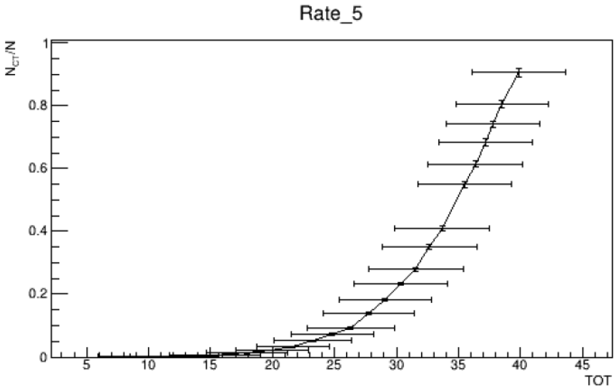

Simulation and data flow

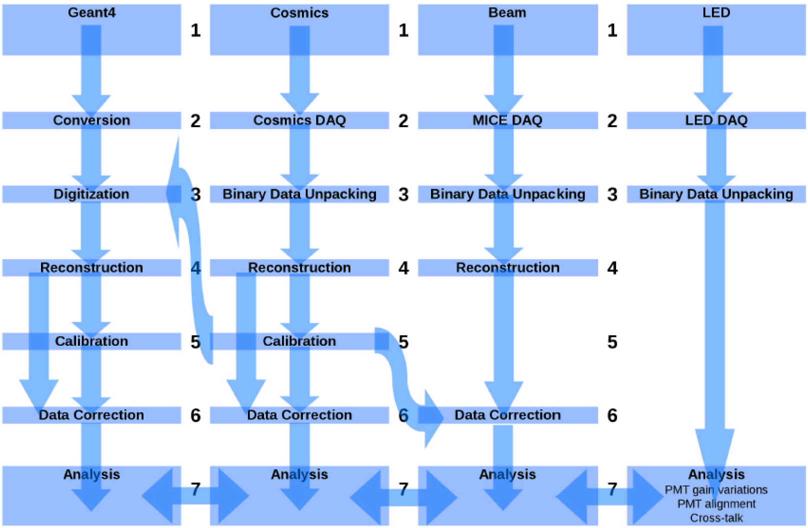

Digitisation

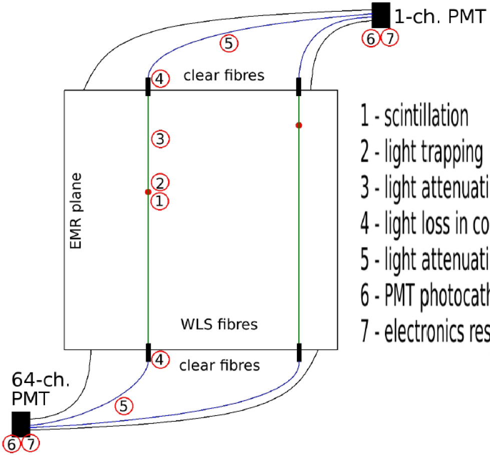

1 - scintillation
2 - light trapping by WLS fibre
3 - light attenuation in WLS fibre
4 - light loss in connector
5 - light attenuation in clear fibre
6 - PMT photocathode
7 - electronics response

Digitisation procedure

All digitization parameters are preliminary

1. convert energy given by Geant4 into the number of scintillation photons (nsph): 2000 photos/MeV
2. sample nsph with Poisson distribution
3. covert nsph to the number of trapped photons (ntph): trapping efficiency 2%
4. sample ntph with Poisson distribution

64-ch. PMT - bar readout

6. reduce ntph according to the length of wavelength shifting fiber (WLSf) and clear fiber (CLf) (naph): WLSf - 2.0 dB/m, CLf - 0.35 dB/m
7. apply channel attenuation map: ight loss in connectors up to 30%
8. sample naph with Poisson distribution
9. convert naph to the number of photoelectrons (npe): PMT quantum efficiency - 20%
10. sample npe with Poisson distribution
11. correct npe for photocathode non-uniformity: up to 40%
12. convert npe to the number of ADC counts: 8 ADC/npe
13. simulate electronics response: gaussian smearing - width 10 ADC
14. convert nADC to TOT: nADC=a+b*log(TOT/c+d)
15. covnert geant4 time to ADC counts (deltaT): 2.5ns/ADC
16. sample deltaT with Gaussian distribution: width - 2 ADC

1-ch. PMT - plane readout

6. reduce ntph according to the length of wavelength shifting fiber (WLSf) and clear fiber (CLf) (naph): WLSf - 2.0 dB/m, CLf - 0.35 dB/m
7. apply channel attenuation map: ight loss in connectors up to 30%
8. sample naph with Poisson distribution
9. convert naph to the number of photoelectrons (npe): PMT quantum efficiency - 14.5%
10. sample npe with Poisson distribution
11. correct npe for photocathode non-uniformity: up to 50%
12. convert npe to the number of ADC counts: 1 ADC/npe
13. simulate electronics response: gaussian smearing - width 6.5 ADC
14. set signal baseline (8bit ADC):~130 ADC
15. simulate noise level - number of fluctuations within acquisition window: from 0 to 200
16. set noise position: upwards/downwards fluctuations
17. simulate negative voltage pulse with random noise

Digitisation: MC Raw → MC Digitised

- 3 GeV muons simulated (to be compared with cosmics)
- left plot: energy deposition per plane in MeV
- right plot: digitized energy after electronics conversion - total charge per plane in ADC counts

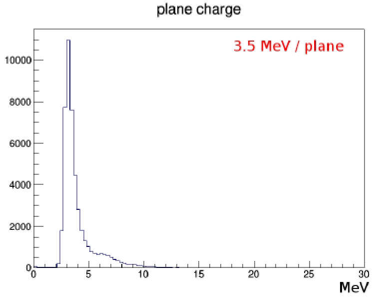

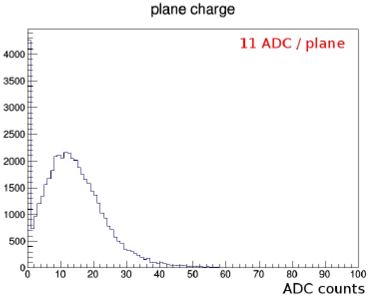

Digitisation: MC Digitised → Cosmics

- 3 GeV muons simulated (to be compared with cosmics)
- left plot: digitized energy after electronics conversion - total charge per plane in ADC counts
- right plot: total charge per plane from cosmic muons

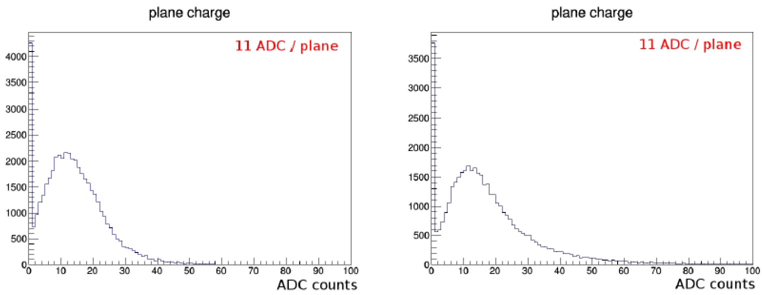

- even with peliminary digitization parameters the agreement is very good

Track reconstruction: Based on Timing

- after cleaning event is ready for track reconstruction

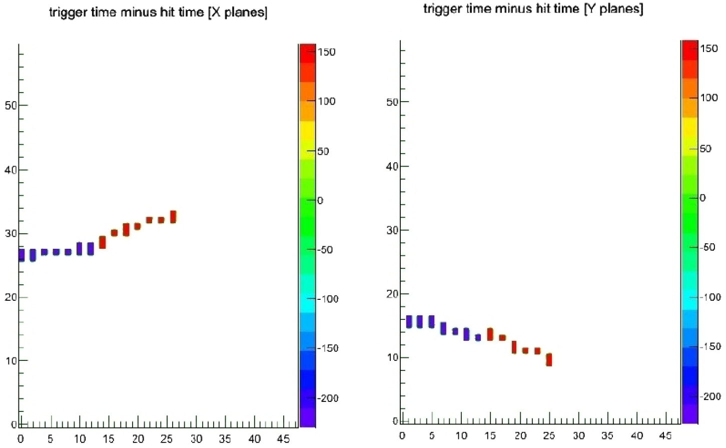

Track reconstruction: Based on Timing

- primary and secondary tracks are easily identified

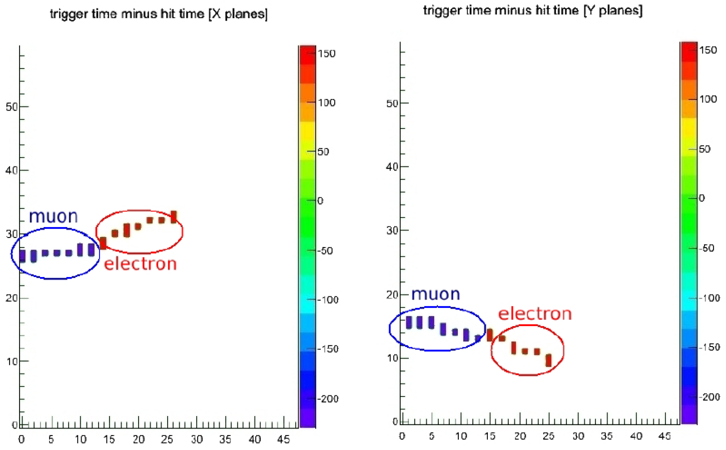

Installed on MICE beamline end September 2013

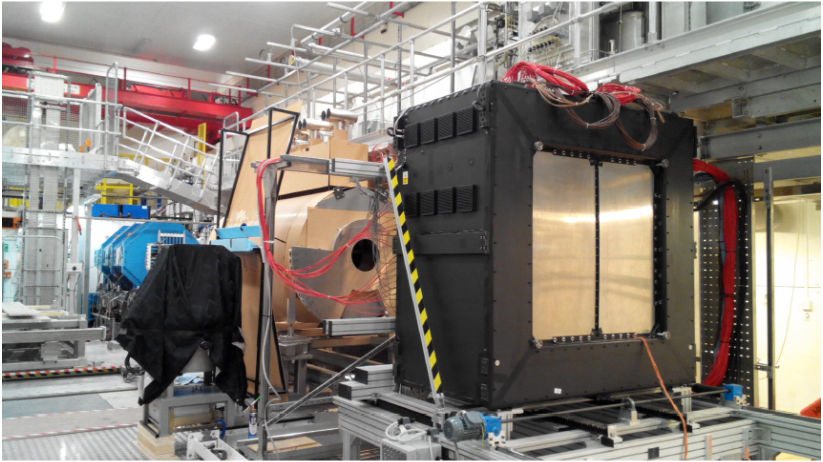

Online operation at RAL: October 2013

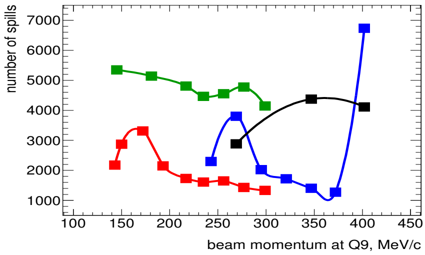

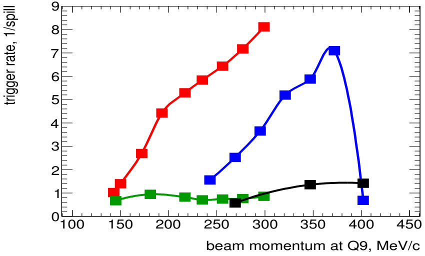

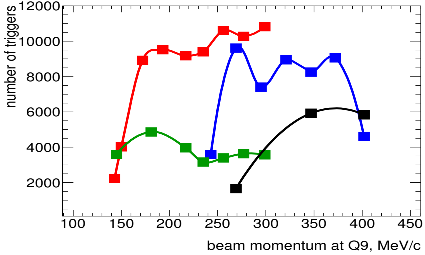

- Red: e^+ beam;
- Blue: π^+ beam;
- Green: e^- beam;
- Black: π^- beam.

EMR reconstructed range: preliminary 1/20th stats

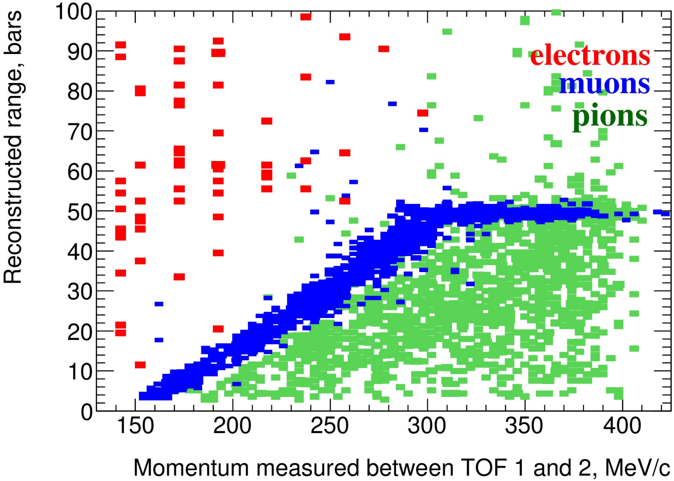

TASD simulations in a B-field: $e/\mu/p$

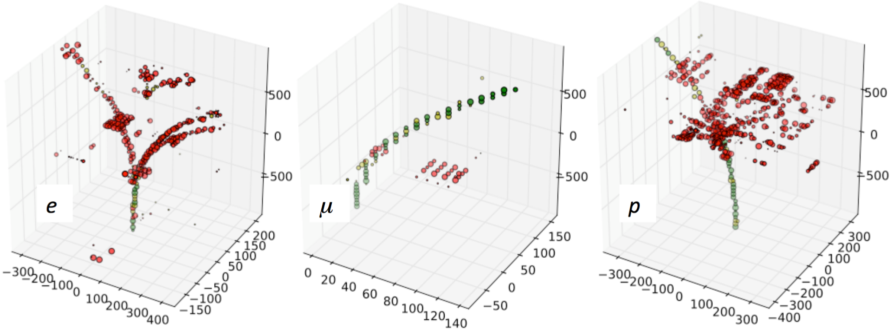

TASD simulations in a B-field: sign of electron: 5 GeV

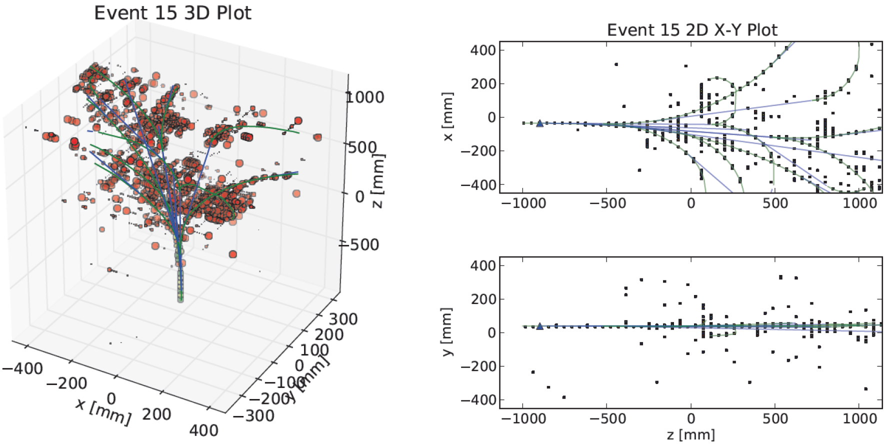

MIND magnetisation options

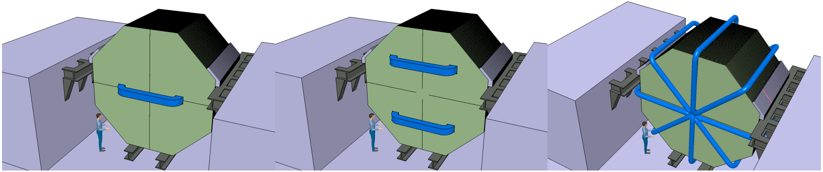

MIND magnetisation: measuring B-field in-situ

- Slit in steel, few mm...
- fill with non-magnetic material (e.g. SS316L);
- Insert probe to measure field at various points along slit;
- Small distortion of field lines;
- Measurements validate simulated field across whole detector;
- 23000 At with slot c.f. 4000 At without slot.

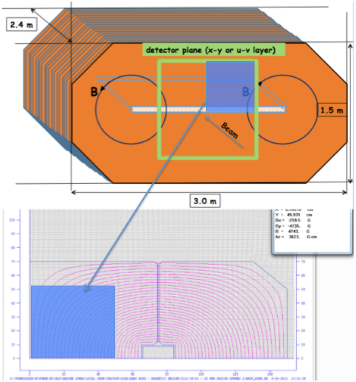

MIND plastic scintillator bars from INR

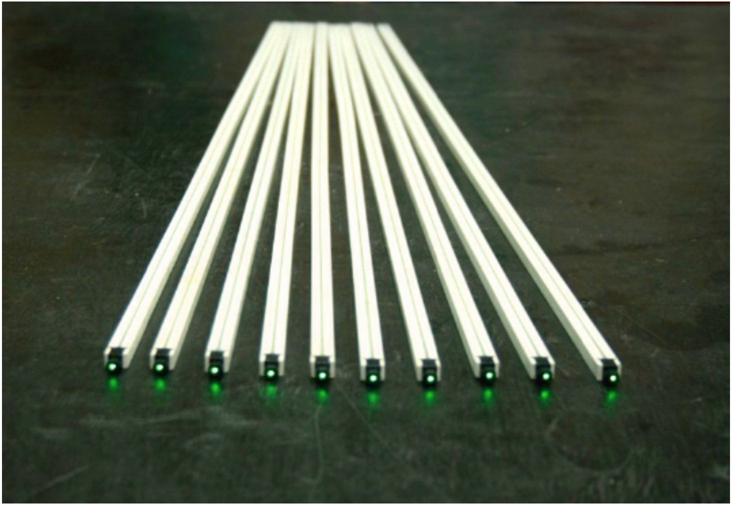

Scintillator bar connector design

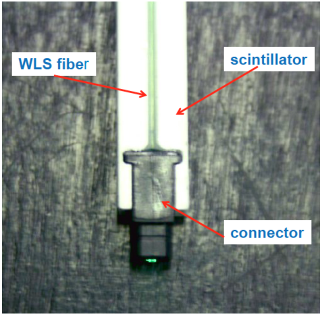

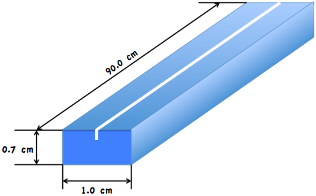

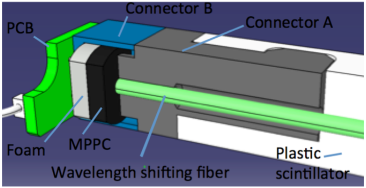

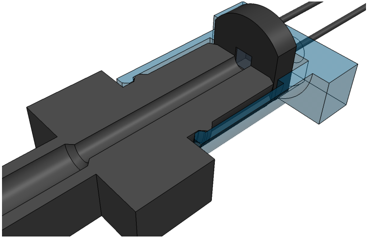

Plastic scintillators tests with cosmics

- Tests carried out to determine basic light yield and timing properties;
- Light collection: Kuraray wavelength shifting fiber, 1.0 mm diameter, $\sim$1 m long, embedded in groove with Toshiba TSF451-50M silicon grease;
- Light readout: SiPM photosensors on both sides;
- Cosmic telescope:
  - two trigger counters;
  - upper one: $7 \times 7\ cm^2$ (L.Y.) and $2 \times 2\ cm^2$ (timing);
  - lower one: $10 \times 24\ cm^2$.
  - measurement at counter center: light yield per MIP.

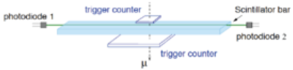

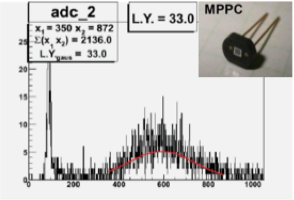

	MPPC
Number of pixels	667
Active area	1.3×1.3 mm^2
Pixel size	50×50 μm^2
Gain	0.7×10^6
PDE at 525 nm	30-35%
Dark rate, thr = 0.5 p.e.,22C	<500 kHz
Pulse width	<100 ns
Cross-talk	10-20%
After pulses	10-20%
Sensitivity to magnetic field	no

Light yield: slabs with chemical reflector

Slab width [mm]	MPPC 1 L.Y. [p.e.]	MPPC 2 L.Y. [p.e.]	$\Sigma_{L.Y.}$ [1+2] [p.e.]
Chemical reflector			
10	46.0	36.8	82.8
20	39.7	35.7	75.4
20	32.6	28.2	60.8
30	31.2	26.6	57.8
Chemical reflector, w/o optical grease			
20 - grease	25.7	22.1	47.8
Chemical reflector + Tyvek paper reflector			
20 + Tyvek	49.3	44	93.3

- $\sim \times$ 2.5 effect of chemical reflector;
- $\sim$ 60 % effect of optical grease;
- $\sim$ 20 % effect of additional Tyvek reflector.

Timing characteristics

- Timing estimation with small 2 × 2 cm^2 upper trigger counter;
- $\sim$ 0.5 p.e. TDC threshold to suppress time-walk effects;
- Two-sided readout $\rightarrow (t_1 - t_2)/2$ to estimate timing;
- Timing is mostly determined by fiber decay constant:
  - $\tau_{fiber} \sim 12$ ns;

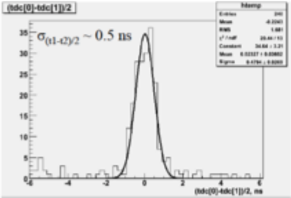

$\sigma_{(t1-t2)/2}$ vs L.Y. according to T2K SMRD test-bench results

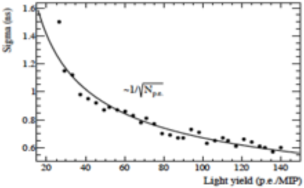

Light yield for the different WLS fibers

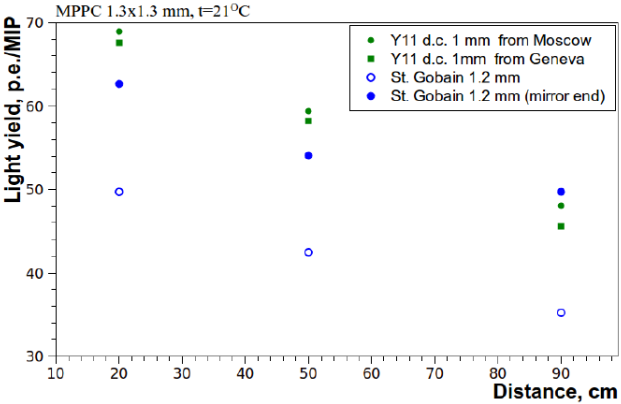

- 3 fibers tested with open end, with cosmic triggers at 20, 50, 90 cm;
- Then one measurement on St. Gobain with Al Mylar mirror on open end.

Parameter	Unit	MPPC-T2K	ASD-40	KETEK	SensL
Manufacturer reported specifications					
Pixel size	μm	50	40	50	20
No. of pixels		667	600	400	848
Sensitive area	mm^2	1.3×1.3	dia 1.2	1.0×1.0	1.0×1.0
Gain		7.5×10^5	1.6×10^6	-	-
Dark rate	MHz	≤ 1	~ 3	≤ 2	≤ 2
Bias voltage	V	~ 70	30-50	33-50	30
Performance					
Overvoltage	V	$\sim$1.4	3.6	4.5	2.7
Dark rate	kHz	900	3630	1250	1960
Crosstalk	%	10	13.4	35	9.7
Pulse shape	-	good	good	long tails	good
Peak separation	-	good	good	bad	bad
PDE	%	25.6	11	26.4	14.2

Photosensor charge spectra

Green LED flash light is sent through a monochromator and collimator to a SiPM.
ADC gate is 150 ns. Wavelength is 520 nm. Temperature is 25^{o}C.

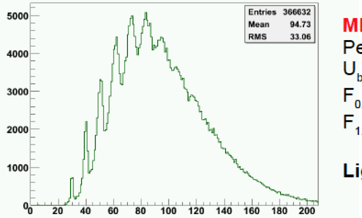

MPPC response to LED signal.
Pedestal and up to 8 p.e. peaks can be separated
U_{bv}=69.2 V (specified by Hamamatsu)
$F_{0.5}$=900 kHz
$F_{1.5}$=90 kHz

Light yield is about 5 p.e.

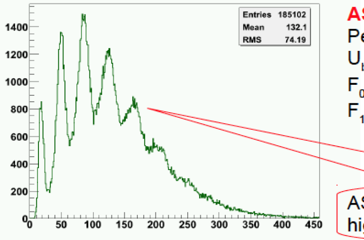

ASD-SiPM1C-40 response to LED signal.
Pedestal and up to 5 p.e. peaks can be separated
U_{bv}=47.2 V (3.6 V overvoltage)
$F_{0.5}$=3630 kHz
$F_{1.5}$=490 kHz

Light yield is about 3 p.e.

ASD sensor produces well separated peaks even at high dark rate

Detector module design

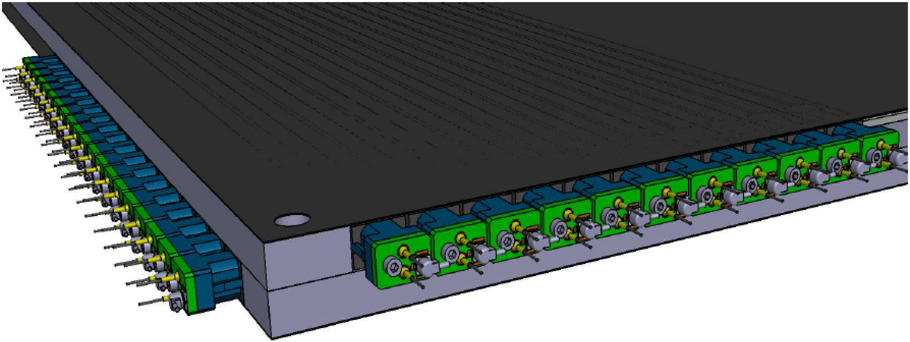

Readout scheme

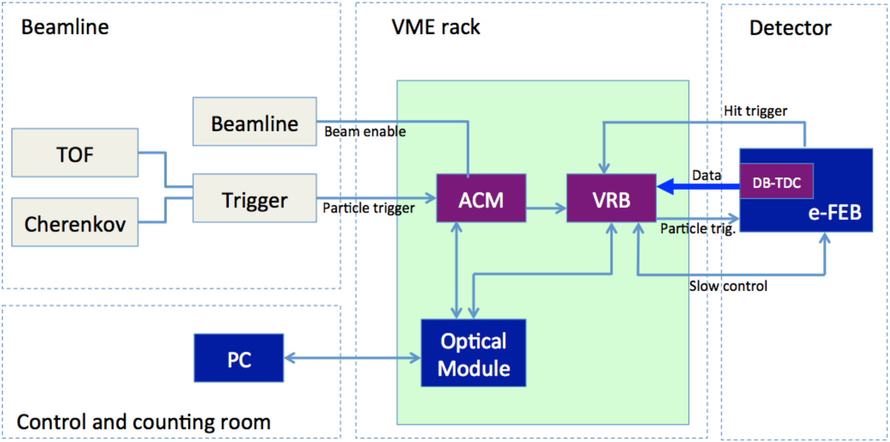

ACM – AIDA Clock Module
VRB - VME Readout Board

DB-TDC – Digitizer Buffer TDC
e-FEB – Easiroc Front End Board

Easiroc schematic and planned charge+hit measurements

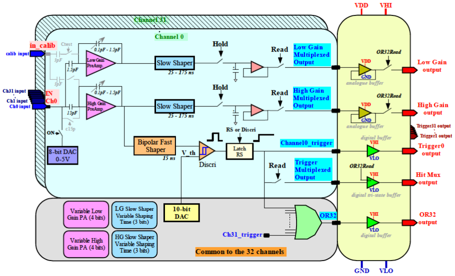

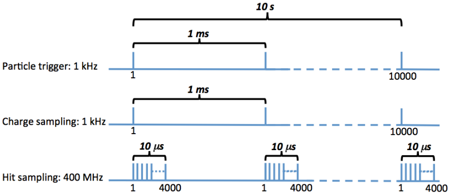

Easiroc tests with latest generation MPPC

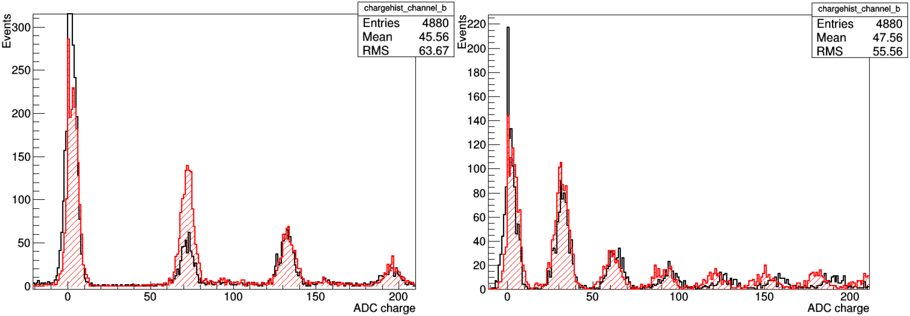

Charge spectra for the MPPC S12571-050C, a 50-micron cell size, 1×1 mm^2 device. Analogue data from the high gain signal path from the EASIROC chip, digitised with a 12-bit ADC, demonstrates the excellent photo-electron peak-to-peak separation. The EASIROC pre-amp feedback capacitance is set to 100fF, the shaper τ is set to 50ns. Left) high over voltage leading to $\sim$ 65 ADC/p.e. Right) low over voltage leading to $\sim$ 30 ADC/p.e. ΔV between left and right acquisitions is 1.75 V.

R. Bayes

MIND Prototype:

- 1 m × 1 m × 2 m.
- 3 cm Fe.
- 2 cm scintillator.
- 7 cm dia. copper STL (for scattering).
- Toroidal B-field 100 kA.

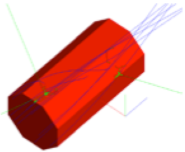

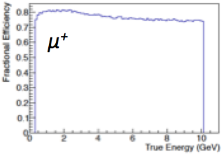

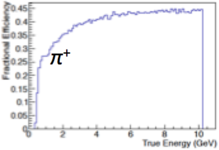

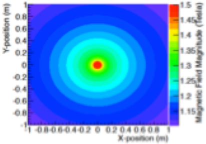

10 μ^+ events ↑:

- Generated at random on X-Y plane at Z=L/2
- 1 million events per simulation

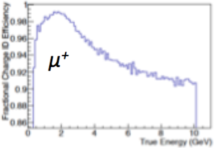

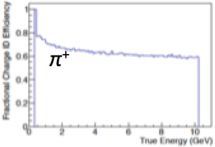

Particle	Detector - MIND	Reconstruction efficiency	Charge identification efficiency
μ^+	Prototype	80% (1GeV) 75% (10GeV)	99% (1GeV) 91% (10GeV)
μ^+	Far	81% (Flat 1 to 25GeV)	99.5% (1GeV) 98% (25GeV)
μ^-	Prototype	60% (1GeV) to 64% (10GeV)	92% (1GeV) to 83% (10GeV)
π^+	Prototype	13% (1GeV) to 45% (10GeV)	80% (1GeV) to 60% (10GeV)
π^-	Prototype	11% (1GeV) to 42% (10GeV)	75% (1GeV) to 55% (10GeV)

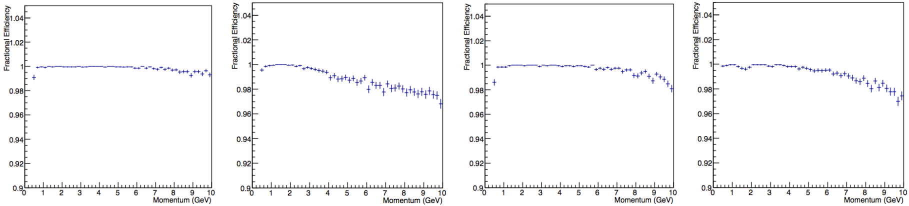

Figure : Reconstruction efficiencies for μ^+, from left: a) 3 cm steel, 1.5 cm scintillator. b) 2 cm/1.5 cm. c) 3 cm/3.5 cm. d) 2 cm/3.5 cm.

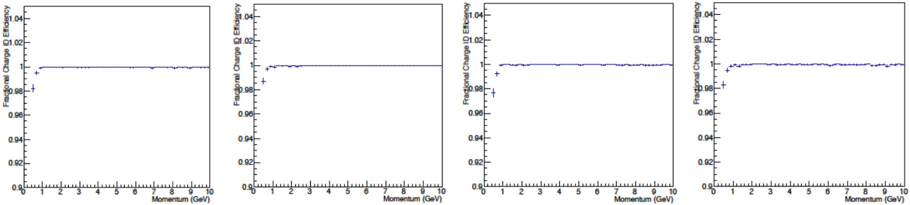

Figure : Corresponding charge identification efficiencies for μ^+.

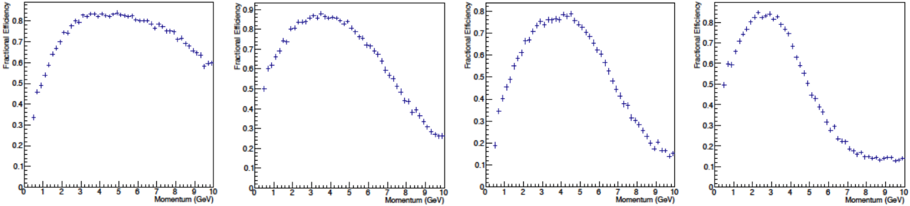

Figure : Reconstruction efficiencies for π^+, from left: a) 3 cm steel, 1.5 cm scintillator. b) 2 cm/1.5 cm. c) 3 cm/3.5 cm. d) 2 cm/3.5 cm.

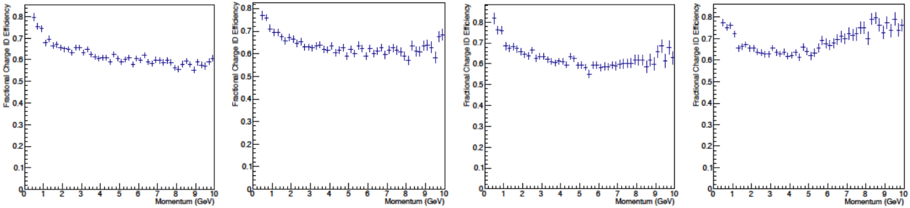

Figure : Corresponding charge identification efficiencies for π^+.

TMVA for the AIDA MIND50

- Muon ID by range done by MIND/SuperBIND absent in MIND50:
  - Muons rarely range out;
  - Need to rely on other PID metrics;
- Existing PID methods could be adapted for PID in AIDA MIND;
  - TMVA-based PID for MICE EMR;
  - Clear differentiation between e, π, μ;
  - Training MIND50 on μ, π, p, e.

Summary

- TASD successfully tested online:
  - Assembled at the University of Geneva;
  - Installed on MICE beamline at RAL September 2013;
  - Detector performance under evaluation;
  - Data analysis ongoing.
- MIND construction underway:
  - Several component choices made (plastic scintillator, WLS fiber, optical glue);
  - Photosensor characterization ongoing for final choice in May;
  - Good progress on manufacturing of scintillator bars by INR;
  - Electronics by UniGe;
  - Steel and magnetisation in collaboration with CERN.
- Outlook for TASD and MIND:
  - Several projects plan such detectors;
  - MIND prototype foreseen for WA105 at CENF.

Acknowledgements

- Thanks to colleagues for supplying material for this talk, R. Asfandiyarov, R. Bayes, A. Blondel, F. Cadoux, Y. Karadzhov, Y. Kudenko, R. Matev, O. Mineev, M. Rayner, P. Soler, T. Stainer, R. Terri, R. Tsenov, ...